ELSEVIER

Journal of Photochemistry and Photobiology A: Chemistry 137 (2000) 87–92

Journal of Photochemistry and Photobiology A:Chemistry

www.elsevier.nl/locate/jphotochem

The spectral shape dependence of xanthone triplet–triplet absorption on solvent polarity

C. Ley, F. Morlet-Savary*, J.P. Fouassier, P. Jacques

Département de Photochimie Générale, CNRS UMR no. 7525 ENSCMu, 3 Rue Alfred Werner, 68093 Mulhouse cedex, France

Received 25 July 2000; accepted 14 September 2000

Abstract

Transient triplet–triplet absorption spectra of xanthone were obtained in several solvents through picosecond pump probe experiments. Shape and wavelength maximum of the absorption spectrum depended on the polarity. The evolution of the wavelength maximum was analyzed in terms of the dielectric continuum theory (Onsager function), the Dimroth empirical parameter $E_T(30)$ and the Kamlet and Taft solvent parameters. In nonpolar solvents transient absorption spectra showed two bands, ascribed to transitions originating from both $^3n\pi^*$ and $^3\pi\pi^*$ excited states. The nature of the lowest excited triplet state was mostly $^3\pi\pi^*$ in polar and $^3n\pi^*$ in nonpolar solvents.

Keywords: Xanthone; Picosecond; Transient absorption; Solvatochromism

1. Introduction

Due to their role in photochemical and photobiological reactions, the triplet states of aromatic ketones continue to receive attention from both experimental and theoretical points of view. It is well known that the polarity of a solvent greatly influences the energies of the electronic states as well as the photophysical properties in aromatic carbonyl systems. Among the aromatic carbonyl compounds, thioxanthone (TX) and xanthone (Xn) are extensively studied from a solvent effect point of view. Generally, an increase in solvent polarity results in the stabilization of the $^3\pi\pi^*$ state and a destabilization of the $^3n\pi^*$ state. For example, thioxanthone shows a dramatic solvent effect upon fluorescence properties and triplet–triplet absorption spectra (TTA) [1–8]. It has been shown that the configuration of the lowest triplet state of these compounds can be correlated with properties such as photochemical reactions and relaxation behavior. In aromatic ketones such as TX and Xn, the small energy gap between configurations $^3n\pi^*$ and $^3\pi\pi^*$ leads to a substantial mixing of these states. As regards Xn, several spectroscopic studies have been performed so far to determine the solvent effect upon the excited triplet states ordering [9–13]. It was generally accepted that the lowest excited triplet state of Xn exhibits a $^3\pi\pi^*$ configuration as revealed by the various spectroscopic measurements carried out in glassy matrices or pure Xn crystal at low temperature [9–13]. These various studies demonstrate that $^3n\pi^*$ and $^3\pi\pi^*$ are close in energy and that the energy gap between singlet and triplet states is very small [9,10,14]. This small energy gap also leads to a level inversion when going from nonpolar to polar solvents [14] where $^3\pi\pi^*$ moves to lower energies as the solvent polarity increases. This change in the ordering was also invoked to explain the Xn phosphorescence behavior at 77 K [9] in glassy matrices, where the lowest triplet state is $^3\pi\pi^*$ in EPA matrix (ethanol isopentane ether 5:2:2) and $^3n\pi^*$ in 3-methylpentane (3-MP).

The Xn triplet state is relatively long lived (several microseconds) in polar solvents, where it exhibits a $\pi\pi^*$ character [14–16] and is not very reactive towards hydrogen atom abstraction [14]. The TTA spectrum of Xn shows a characteristic blue shift when the solvent polarity is increased, e.g. the absorption maximum is 648 nm in carbon tetrachloride, 616 nm in 2-propanol and 580 nm in water [17]. At this point, it should be noticed that the width and the shape of the triplet–triplet absorption (TTA) spectrum evolves with the solvent polarity [17]. This blue shift solvatochromy may be related to dipole moment variations which occurs during the triplet–triplet transition. The dipole moment values found in the literature are 3.1 D [18] and 5.1 D [4] for the ground and first excited singlet states, respectively, and 3.51 D for the excited triplet state T_n [4], derived from TTA nanosecond studies.

* Corresponding author.
E-mail address: f.morlet-savary@univ-mulhouse.fr (F. Morlet-Savary).

1010-6030/00/$ – see front matter
PII: S1010-6030(00)00374-9

The xanthone molecule is also characterized by a high intersystem crossing (ISC) quantum yield, whose value is 0.97 at room temperature [14]. The ISC rate constants determined from picosecond and more recently from femtosecond experiments are in the 10 ps range [19–21]. These results have been confirmed by Scaiano et al. [22] who have found that the singlet state lifetimes of xanthone in acetonitrile and 2-propanol are less than the resolution of the apparatus (<30 ps). From these behaviors in solvent medium, Scaiano et al. proposed to use the xanthone molecule as a microenvironment sensor [17] and to study the multistage exit of excited xanthone from micelles or cyclodextrins [23]. For this purpose, a calibration of the TTA of Xn as a function of solvent parameters has also been suggested [17]. The present study will be focused on the analysis of triplet–triplet absorption spectra of Xn in several solvents through picosecond pump probe experiments. This particular technique allows recording of TTA spectra (i) with higher resolution, (ii) shortly after the excitation pulse (500 ps) avoiding furthermore the transient absorption of other species like Xn ketyl radical. A discussion of the solvatochromism of Xn and the spectral shape in terms of solvent parameters will be considered by determining the number of transitions occurring in the absorption band through the simulation of these well resolved TTA.

2. Experimental

2.1. The pump probe picosecond apparatus

The picosecond set-up is based upon the classical pump-probe spectroscopic arrangement and has already been described in some detail [7]. In short, the idea consists in using a short exciting laser pulse (pump pulse) to create a transient species and analyzing the absorption of this state with a white light pulse (probe pulse), so that an absorption spectrum could be recorded at each laser pulse. The picosecond pulses were delivered by a passively–actively mode locked Nd:YAG laser (BM Industries). The fundamental (1064 nm) and the third harmonic (355 nm) emission were used to generate the white light continuum probe from the D_2O/H_2O mixture and to excite the sample in solution, respectively. The white light was collected and, then, collimated by a set of achromatic lenses, sent onto a large band beamsplitter to illuminate both sample and reference cell. The transmitted light was focused by appropriate lenses and injected into fiber optics directly connected to the dispersive element (Jobin Yvon CP 200) of the double diode arrays multichannel analyzer (Princeton Instruments ST 121 controler and DDA1024 detector). The solution was flowed through two cells (2 mm optical pathlength) the reference one (non excited) and the sample one (excited). A delay of up to 6 ns could be achieved between the pump and the probe pulses by using a computer-controlled micrometer translation stage. The laser excitation energy was ca 250 μJ while the excitation area was 2 mm across, the probe one was 1 mm. The pulse width σ was ca. 25 ps under the experimental conditions and the time resolution less than 10 ps.

2.2. Analysis of the transient spectra

The frequencies of the absorption band in the transient spectra were determined by fitting the spectra to a function $\varepsilon(\nu)$ determining a series of log–normal line shapes, as defined by [24]

$$\varepsilon(\nu) = \begin{cases} \varepsilon_0 \exp\left[-\ln 2\left(\frac{1}{\beta}\ln\left[1+\frac{2\beta(\nu-\nu_0)}{\Delta}\right]\right)^2\right] & \text{if } \alpha > -1 \\ 0 & \text{if } \alpha \leq -1 \end{cases}$$

where

$$\alpha = \frac{2\beta(\nu-\nu_0)}{\Delta}$$

This function describes an asymmetric line shape which reduces to a Gaussian shape function at the boundary $\beta = 0$. Parameters ε_0, ν_0, β and Δ are the peak height, peak frequency (cm^{-1}), asymmetry parameter and spectral bandwidth, respectively.

2.3. Chemicals

Xanthone (Xn) (9H-xanthen-9-one, CAS no.: 90-47-1) was purchased from Fluka (puriss. p.a.) and used as received. All the solvents were of spectrophotometric grade. All the experiments were carried out in argon saturated solution unless otherwise mentioned.

3. Results and discussion

After absorption of light, Xn was brought up to its first excited singlet state, from which an ultrafast intersystem crossing drops the molecule in its triplet excited state [21]. Fig. 1 shows the T_1–T_n spectra of Xn in toluene (Tol), tetrahydrofurane (THF), ethylacetate (EtAc), acetonitrile (MeCN) and methanol (MeOH). It should be noted that these absorption spectra are nearly free of noise and spectrally very well resolved (<5 nm). This enables location of the maximum with a much better precision than with conventional nanosecond laser flash spectroscopy. All spectra were taken 500 ps after the pump pulse: at this time all the solvation processes were terminated. In addition these triplet–triplet absorption maxima are in good agreement with the values derived from nanosecond laser flash spectroscopy experiments [4,17] (see Table 1). What is more, at this time no ketyl radical arising from the triplet state was detectable (in hydrogen donating solvents), which makes it possible to observe triplet state absorbance only in the 400–800 nm range. The absorption maximum shifts towards shorter wavelengths as the polarity

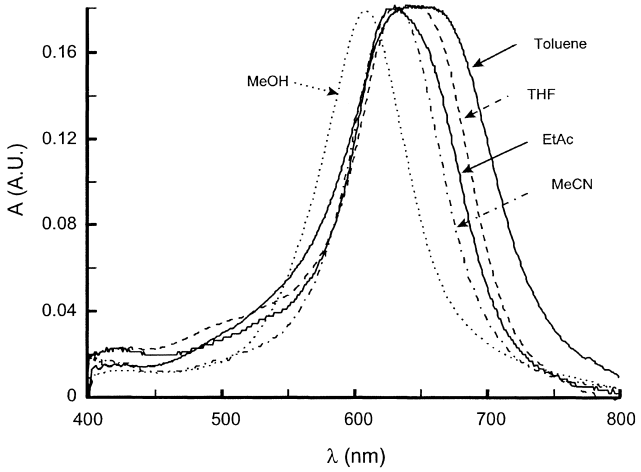

Fig. 1. Normalized absorption band of picosecond TTA spectra of xanthone in toluene, THF, EtAc, MeCN and MeOH.

of the medium increases (Fig. 1): from 647 nm in toluene to 606 nm in MeOH. The solvatochromism of the Xn TTA seems, however, to be less substantial between nonpolar/polar solvents than between polar/hydroxilic solvents. While the shift of the absorption maximum between MeCN ($\lambda_{max} = 631$ nm) and toluene ($\lambda_{max} = 647$ nm) is ca. 16 nm, the shift between MeOH ($\lambda_{max} = 606$ nm) and MeCN is ca. 25 nm, which may suggests the possible role of specific interactions in the solvatochromism of Xn triplet state. The main fact is that the shape of the absorption band changes with the medium polarity. On one hand, Fig. 1 shows that, in nonpolar solvents like toluene/cyclohexane and in slightly polar (non hydroxylic) solvents like EtAc and THF, the T_1–T_n absorption band is very large. On the other hand, in

Table 1
Xanthone triplet absorption maximum (λ_{max}) from present work and from [4,17] as a function of the solvent[a]

Solvent	λ_{max} (nm)		
	Present work	[17]	[4]
Cyclohexane	623		
CCl_4	648	648	
Benzene		649	655
Toluene	647		
Diethyether	624		
Dioxane		642	
Tetrahydrofuran	641		
Ethylacetate	629	628	
DMF	645		
Acetonitrile	631	627	635
2-Propanol	618	616	
1-Butanol	617		
1-Propanol	616		
Ethanol	613		610
Methanol	606	605	610
Ethyleneglycol	608	601	

[a] DMF: dimethylformamide.

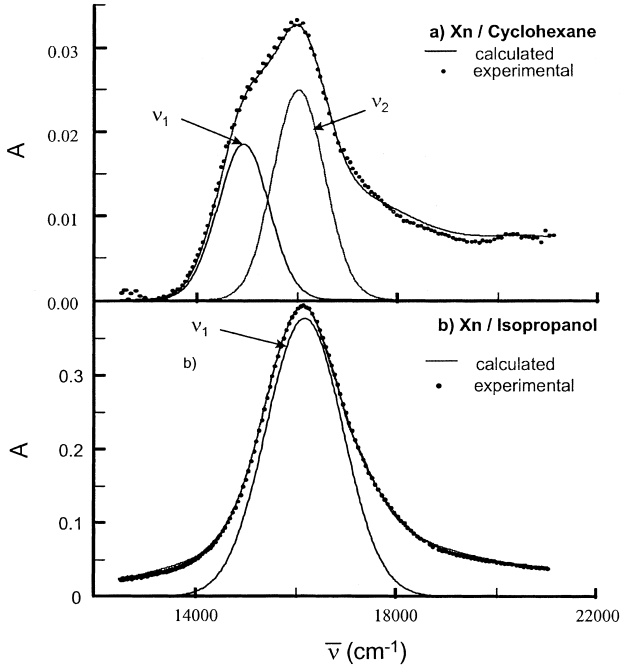

Fig. 2. Reconstruction of picosecond TTA spectra of Xn in (a) a nonpolar solvent (cyclohexane) and (b) a polar solvent (MeCN).

polar and polar/hydroxylic solvents the bandwidth decreases (see MeCN and MeOH in Fig. 1) as already reported in [17].

Additional insight into the solvatochromism of Xn can be expected by determining the number of transitions occurring in the absorption band. For this purpose, a sum of log–normal functions was used to reconstruct the spectra. Fig. 2 shows the experimental and the calculated TTA spectra of Xn in MeCN and cyclohexane. While two main bands defined by $\bar{\nu}_1$ and $\bar{\nu}_2$ were needed to correctly describe the experimental data in the nonpolar solvents (e.g. cyclohexane), only one band was needed in MeCN. For solvents no. 1–7, two log–normal functions were required to simulate the TTA spectra, whereas for solvents no. 8–13 only, one function characterized by $\bar{\nu}_1$ was needed. The peak positions of the extracted transition in the different solvents are listed in Table 2: $\bar{\nu}_1$ corresponds to the less energetic transition (the "red" one) and $\bar{\nu}_2$ to the more energetic (the "blue" one). As shown below, the solvatochromisms of these two transitions are widely different: the dependence of $\bar{\nu}_1$ on polarity is higher than that of $\bar{\nu}_2$. It is apparent that in polar and hydroxylic solvents the latter band ($\bar{\nu}_2$) disappears while the former ($\bar{\nu}_1$) shifts to shorter wavelengths (vide infra).

The description of solute–solvent interactions requires a distinction between normal (dipolar) and specific interactions (like hydrogen bonding). Normal solute–solvent interactions involve multipole and polarisability properties of both solute and solvent molecules. These interactions are mainly described by the dielectric continuum model. The solvents are characterized by their static dielectric constant *D* and their refractive index *n* through the Onsager polarity functions [25,26]

Table 2
Solvent parameters and frequency maximum from calculated spectra $\bar{\nu}_1$ and $\bar{\nu}_2$ (cm^{-1})[a]

Serial no.	Solvent	$E_T(30)$ (kcal mol^{-1})	n	D	π^*	α	ν_1 (cm^{-1})	ν_2 (cm^{-1})
1	Cyclohexane	30.9	1.426	2.02	0.00	0.00	14950	16045
2	CCl_4	32.4	1.460	2.24	0.28	0.00	14940	16120
3	Toluene	33.9	1.497	2.38	0.54	0.00	15080	16270
4	Diethyether	34.5	1.353	4.27	0.27	0.00	15000	16070
5	Tetrahydrofuran	37.4	1.405	7.52	0.58	0.00	15190	16181
6	Ethylacetate	38.1	1.372	6.08	0.55	0.00	15300	16250
7	DMF	43.8	1.428	36.71	0.89	0.00	15550	16120
8	Acetonitrile	45.6	1.344	35.94	0.75	0.19	15930	
9	2-Propanol	49.2	1.377	19.92	0.48	0.76	16200	
10	1-Butanol	50.2	1.399	17.51	0.47	0.84	16220	
11	1-Propanol	50.7	1.386	20.45	0.52	0.84	16270	
12	Ethanol	51.9	1.361	24.55	0.54	0.86	16340	
13	Methanol	55.4	1.328	32.66	0.60	0.98	16520	
14	Ethyleneglycol	56.3	1.432	37.70	0.92	0.90	16430	

[a] $E_T(30)$, π^* and α from [30]; n, D from [31]. DMF: dimethylformamide.

$$f(D) = \frac{2(D-1)}{2D+1}, \qquad f(n^2) = \frac{2(n^2-1)}{2n^2+1}$$

In the case, where the major solute–solvent interactions arise from dipolar interactions, the overall solvatochromic shift between solvents 1 and 2 can be written as [27,28]

$$(\Delta E_{ge})_{1-2} = -\vec{\mu}_g(\vec{\mu}_e - \vec{\mu}_g)a^{-3}\left[f(D) - f(n^2)\right]_{1-2}$$

where ΔE_{ge} is the solvation energy difference between a relaxed initial state (g) (with dipolar moment μ_g) and a Franck–Condon final state (e) (with dipolar moment μ_e), a is the radius of Onsager's cavity.

This approach excludes, however, specific solute–solvent interactions like hydrogen bonding. Thus, in the case of hydroxylic solvents, empirical polarity scales must be used. Among the overabundance of existing empirical methods, two well-known approaches were chosen: (i) the empirical polarity parameter of Dimroth $E_T(30)$ (based upon the UV transition solvatochromism of a betaine dye [29–32]); (ii) a semi-empirical method (multilinear approach), called the solvatochromic comparison method (SCM) which characterizes the solvent by three principal parameters [32–35]: π^* (an index of solvent polarity/polarisability which measures the ability of the solvent to stabilize a dipole by virtue of its dielectric properties), α (the ability of the solvent to donate a hydrogen bond to the solute) and β (the ability of the solvent to accept a hydrogen bond from the solute). Thus, the evolution of a property XYZ with the solvent will be linked to these three parameters by a linear relationship (linear solvation energy relationship, LSER)

$$XYZ = XYZ_0 + s\pi^* + a\alpha + b\beta$$

where XYZ and XYZ_0 are the investigated properties in the solvent and the gas phase, respectively.

The evolution of $\bar{\nu}_1$ (squares) and $\bar{\nu}_2$ (circles) with the Onsager's polarity function $[f(D) - f(n^2)]$ is shown in Fig. 3 where the lines are the calculated linear regression for solvents 1–7. It results, therefrom, that the continuum dielectric model fails to explain the solvatochromism of $\bar{\nu}_1$ when all the solvents are taken into account. It is possible to find a linear relationship between $\bar{\nu}_1$ and $[f(D) - f(n^2)]$ only for nonhydroxylic solvents. In hydroxylic solvents (filled squares) the solvatochromism is more significant than predicted by the dielectric continuum model, due to the formation of hydrogen bonds between solute and solvent molecules. Thus, in normal dipolar solvents (no. 1–7), both $\bar{\nu}_1$ and $\bar{\nu}_2$ follow a linear relationship with Onsager's polarity function. In addition, $\bar{\nu}_1$ is much more sensitive to solvent polarity than $\bar{\nu}_2$. This fact may be a consequence of the different nature of the triplet state from which the two observed transitions occur: namely, $\bar{\nu}_1$ originates from $^3\pi\pi^*$ and $\bar{\nu}_2$ from $^3n\pi^*$. It is worthwhile to compare these results with the solvatochromic blue shift of a closely related molecule, thioxanthone, where the $\pi\pi^*$ triplet state

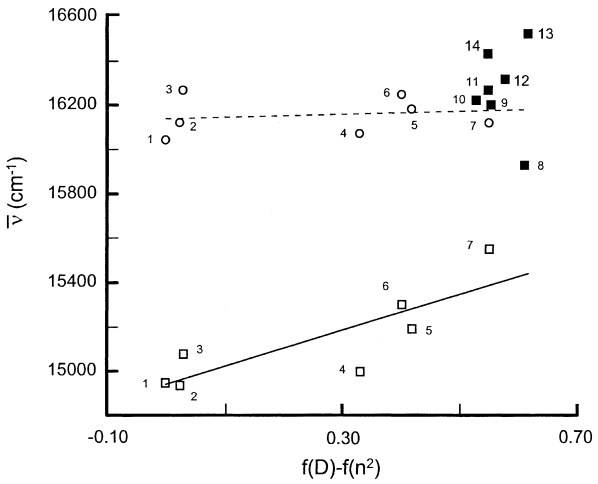

Fig. 3. Evolution $\bar{\nu}_1$ and $\bar{\nu}_2$ with Onsager's polarity function $[f(D) - f(n^2)]$. Failure of the dielectric continuum model to explain the shift of $\bar{\nu}_1$ in hydroxylic solvents. ($\bar{\nu}_2$) Open circles; ($\bar{\nu}_1$) squares (filled squares stand for $\bar{\nu}_1$ in hydroxylic solvents).

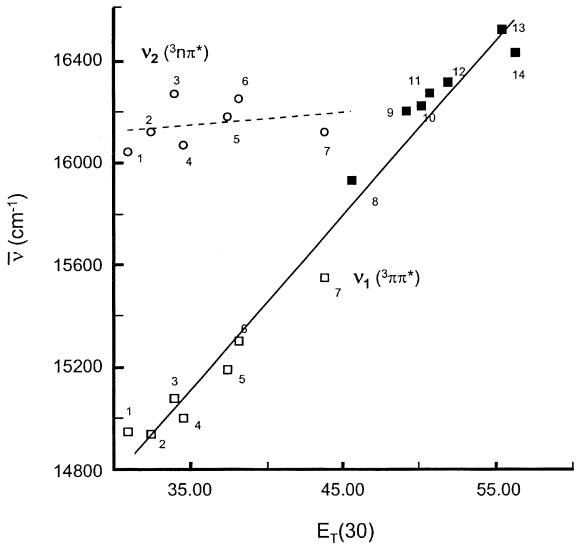

Fig. 4. $\bar{\nu}_1$ and $\bar{\nu}_2$ dependence on the Dimroth empirical polarity parameter $E_T(30)$. ($\bar{\nu}_2$) Open circles; ($\bar{\nu}_1$) squares (filled squares stand for $\bar{\nu}_1$ in hydroxylic solvents).

solvatochromy was found to be very sensitive to the polarity and the hydrogen bonding ability of solvents [7].

The role played by specific interaction like hydrogen bonding is confirmed by Fig. 4 which shows the dependence of both $\bar{\nu}_1$ and $\bar{\nu}_2$ on the Dimroth empirical parameter $E_T(30)$. In solvents where two different bands $\bar{\nu}_1$ and $\bar{\nu}_2$ appear, $\bar{\nu}_2$ is slightly dependent on $E_T(30)$ whereas a very good linear relationship exists between $\bar{\nu}_1$ and $E_T(30)$ for all the solvents used

$$\bar{\nu}_1 = (12717 \pm 135) + (69 \pm 3)\, E_T(30)$$

where r is the correlation coefficient ($r = 0.988$) and n the number of experimental data used to perform the calculation ($n = 14$).

In solvents 1–7, the lowest lying triplet state presumably exhibits a $n\pi^*$ character as already stated in the case of CCl_4 [16]. When going to acetonitrile, isopropanol and methanol, the energy increase of this state (due to the hydrogen bonding) and the energy decrease of the $\pi\pi^*$ state (stabilized by polarity/specific interactions) lead to an inversion of the $\pi\pi^*$ and $n\pi^*$ levels (Scheme 1) in a way similar to that

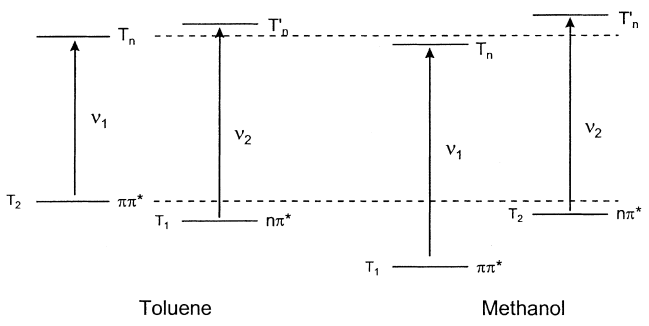

Scheme 1.

postulated in [16] for a mixture of CCl_4 and isopropanol. As a consequence, if the first excited triplet state of Xn in nonpolar solvents is mainly of $n\pi^*$ character, in very polar hydroxylic solvent it acquires $\pi\pi^*$ character, leading to a decrease in photochemical reactivity regarding hydrogen abstraction [16]. Thus, the present spectroscopic study is in good agreement with the results based on the chemical reactivity of Xn and confirms the inversion which occurs in this molecule with increasing polarity. In addition, in polar and hydroxylic solvents, the $^3n\pi^*$ state has a higher energy than the $^3\pi\pi^*$ state and, consequently, is less populated due to the thermodynamical equilibrium. Also, El Sayed's rules should play a non negligible role, since the the lowest singlet of Xn is of $n\pi^*$ configuration. Therefore, the second band ($\bar{\nu}_2$) is no longer observed in polar/hydroxylic solvents.

As $E_T(30)$ is a global polarity parameter of the solvent, that takes into account all possible solute–solvent interactions, especially specific interactions, the results shown in Fig. 4 confirm the influence of hydrogen bonding on the solvatochromism of $\bar{\nu}_1$. Nevertheless, this empirical approach did not shed any light on the different interactions responsible for the $\bar{\nu}_1$ shift. Therefore, the SCM applied to the present data to extract the predominant interaction in the Xn solvatochromy. This multilinear regression led to the following relationship

$$\bar{\nu}_1 = (14924 \pm 92) + (693 \pm 154)\pi^* + (1165 \pm 88)\alpha$$

where $r = 0.981$ and $n = 12$.

Toluene (aromatic) and CCl_4 (chlorinated) were ruled out, because such solvents need additional parameters to be well characterized (see [33]). Parameter β has no influence on the shift of $\bar{\nu}_1$ in agreement with the fact that Xn can accept a hydrogen bond from the solvent, but cannot donate a hydrogen bond to the solvent. Coefficient a of parameter α in the equation is nearly 1.7 times coefficient s of parameter π^*, which means that specific interactions are more efficient than normal (dipolar) solute–solvent interactions in shifting $\bar{\nu}_1$, thus confirming the importance of hydrogen bonding in the solvatochromism of the Xn triplet state.

4. Conclusion

The solvatochromism of the Xn triplet state involves two transitions, originating from the two closely lying triplet states: $^3n\pi^*$ and $^3\pi\pi^*$. The present results reveal that $\bar{\nu}_2$ is very slightly blue-shifted when the polarity increases and probably corresponds to the $^3n\pi^*$ triplet state of Xn. Conversely, $\bar{\nu}_1$, is very sensitive to both solvent polarity and hydrogen bonding and corresponds to the $^3\pi\pi^*$ triplet state of Xn. In addition, when the polarities of the solvents are sufficiently high, the two transitions overlap. When the polarity is highest, the triplet state exhibits a more pronounced $\pi\pi^*$ character. This is a proof of the "inversion" of the two triplet state of Xn with polarity, and this study is in good agreement with Scaiano's paper, where this inversion

of the nature of the Xn triplet state was observed indirectly through a dramatic change in reactivity of the triplet state as regards hydrogen abstraction as the polarity of the medium was increased. At least, the fact that the blue shift for $\bar{\nu}_1$ exceeds that for $\bar{\nu}_2$ by a factor of 10 (1400 versus $100\,cm^{-1}$) also explains why the band shape of the T_1–T_n spectra becomes narrower with increasing polarity: as $\bar{\nu}_1$ shifts towards shorter wavelengths and $\bar{\nu}_2$ becomes less intense, the overall absorption bands becomes narrower.

References

[1] J.C. Dalton, F.C. Montgomery, J. Am. Chem. Soc. 96 (1974) 6230.
[2] T. Lai, E.C. Lim, Chem. Phys. Lett. 73 (1980) 244.
[3] T. Lai, E.C. Lim, Chem. Phys. Lett. 84 (1981) 303.
[4] K.A. Abdullah, T.J. Kemp, J. Photochem. 32 (1986) 49.
[5] D. Burget, P. Jacques, J. Chim. Phys. 88 (1991) 675.
[6] D. Burget, P. Jacques, J. Lumin. 54 (1992) 177.
[7] F. Morlet-Savary, C. Ley, P. Jacques, F. Wieder, J.P. Fouassier, J. Photochem. Photobiol. A: Chem. 126 (1999) 7.
[8] C. Ley, F. Morlet-Savary, P. Jacques, J.P. Fouassier, Chem. Phys. 255 (2000) 335.
[9] H.J. Pownall, J.R. Huber, J. Am. Chem. Soc. 93 (1971) 6429.
[10] A. Chakraborty, N. Hirota, J. Phys. Chem. 80 (1976) 2966.
[11] M. Koyanagi, T. Terada, K. Nakashima, J. Chem. Phys. 89 (1988) 7349.
[12] H.J. Griesser, R. Bramley, Chem. Phys. Lett. 83 (2) (1981) 287.
[13] R.E. Connors, W.R. Christian, J. Phys. Chem. 86 (1982) 1524.
[14] J.C. Scaino, J. Am. Chem. Soc. 102 (1980) 7747.
[15] A. Garner, F. Wilkinson, J. Chem. Soc., Faraday Trans. II 73 (1977) 222.
[16] M. Barra, C. Bohne, J.C. Scaiano, J. Am. Chem. Soc. 112 (1990) 8075.
[17] C.H. Evans, N. Prud'Homme, M. King, J.C. Scaiano, J. Photochem. Photobiol. A: Chem. 121 (1999) 105.
[18] A.L Mc Clellan, Tables of Experimental Dipole Moments, Freeman, San Francisco, 1963.
[19] D.E. Damschen, C.D. Merritt, D.L. Perry, G.W. Scott, L.D. Talley, J. Phys. Chem. 82 (1978) 2268.
[20] B.I. Greene, R.M. Hochstrasser, R.B. Weisman, J. Chem. Phys. 70 (1979) 1247.
[21] J.J. Cavaleri, K. Prater, R.M. Bowman, Chem. Phys. Lett. 259 (1996) 495.
[22] N. Mohtat, F.L. Cozens, J.C. Scaiano, J. Phys. Chem. B 102 (1998) 7557.
[23] M. Barra, C. Bohne, J.C. Scaiano, Photochem. Photobiol. 54 (1) (1991) 1.
[24] D.B. Siano, D.E. Metzler, J. Chem. Phys. 51 (1969) 1856.
[25] C.J.F. Bötcher, P. Bordewijk, Theory of Electric Polarization, Vol. I, Elsevier, Amsterdam, 1977.
[26] H. Frölich, Theory of Dielectrics, 2nd Edition, Oxford University Press, Oxford, 1958.
[27] P. Suppan, Solvatochromism, The Royal Society of Chemistry, 1997.
[28] P. Suppan, J. Photochem. Photobiol. A: Chem. 50 (1990) 293.
[29] C. Reichardt, Solvent and solvent effects in chemistry, VCH, Weinhiem, 1988.
[30] Y. Marcus, Chem. Soc. Rev. (1993) 409.
[31] J.A. Riddick, W.B. Bunger, T.K. Sakano, Organic Solvents, Wiley, New York, 1986.
[32] M.J. Kamlet, J.M.L. Abboud, M.H. Abraham, R.W. Taft, J. Org. Chem. 48 (1983) 2877.
[33] M.J. Kamlet, R.W. Taft, J. Am. Chem. Soc. 98 (1976) 377.
[34] R.W. Taft, M.J. Kamlet, J. Am. Chem. Soc. 98 (1976) 2886.
[35] M.J. Kamlet, C. Dickinson, R.W. Taft, Chem. Phys. Lett. 77 (1) (1981) 69.